PHYSICAL REVIEW D VOLUME 51, NUMBER 1 1 JANUARY 1995

New constraints on supergravity models from $b \to s\gamma$

Jorge L. Lopez,[1,2] D. V. Nanopoulos,[1,2,3] Xu Wang,[1,2] and A. Zichichi[4]
[1] *Center for Theoretical Physics, Department of Physics, Texas A&M University, College Station, Texas 77843-4242*
[2] *Astroparticle Physics Group, Houston Advanced Research Center (HARC), The Mitchell Campus, The Woodlands, Texas 77381*
[3] *CERN Theory Division, 1211 Geneva 23, Switzerland*
[4] *CERN, 1211 Geneva 23, Switzerland*
(Received 5 July 1994)

We perform a detailed study of the constraints from $b \to s\gamma$ on a large class of supergravity models, including generic four-parameter supergravity models, the minimal SU(5) supergravity model, and SU(5)×U(1) supergravity. For each point in the parameter spaces of these models we obtain a range of $B(b \to s\gamma)$ values which should conservatively account for the unknown next-to-leading-order QCD corrections. We then classify these points into three categories: "excluded" points have ranges of $B(b \to s\gamma)$ which do not overlap with the experimentally allowed range, "preferred" points have $B(b \to s\gamma)$ ranges which overlap with the standard model prediction, and "okay" points are neither "excluded" nor "preferred" but may become "excluded" should new CLEO data be consistent with the standard model prediction. In *all* cases we observe a strong tendency for the "preferred" points towards one sign of the Higgs mixing parameter μ. For the opposite sign of μ there is an upper bound on $\tan\beta$: $\tan\beta \lesssim 25$ in general, and $\tan\beta \lesssim 6$ for the "preferred" points. We conclude that new CLEO data will provide a decisive test of supergravity models.

PACS number(s): 13.40.Hq, 04.65.+e, 12.10.Dm, 12.60.Jv

I. INTRODUCTION

Following the precise verification of the unification of the gauge couplings in supergravity unified models [1], there has been a rekindling of interest in low-energy supersymmetric models and their experimental consequences. Supersymmetry can be tested in high-energy collider experiments through the direct production of supersymmetric particles, and in dedicated low-energy experiments through the precise measurement of rare standard model loop-level processes. Because of the large energies required to produce real supersymmetric particles, high-precision experiments are likely to explore the parameter space of supersymmetric models in a much deeper although indirect way for some time to come. In the context of B physics, and the $b \to s\gamma$ process in particular, there appear to be great prospects for a thorough study of this mode by the CLEO Collaboration at the upgraded Cornell Electron Storage Ring (CESR) facility and at planned B factories at SLAC and KEK.

At present there is an experimental upper bound $B(b \to s\gamma) < 5.4 \times 10^{-4}$, and the observation of the $B \to K^*\gamma$ process imposes a conservative lower bound $B(b \to s\gamma) > 0.6 \times 10^{-4}$ [2]. More precise measurements are expected to be announced soon. Despite the availability of precise experimental data, the large [3] and only partially calculated [4] QCD corrections to this process make it unclear [5–7] that one can use the data effectively to test the standard model or constrain models of new physics. Nonetheless, two alternatives appear possible: either the data deviate greatly from the standard model prediction or the data agree well with the standard model prediction. Since supersymmetric models predict a wide range of $b \to s\gamma$ rates (above and below the standard model prediction) [8–16] in either case important restrictions on the parameter space will follow.

Generic low-energy supersymmetric models, such as the minimal supersymmetric standard model (MSSM), are plagued by a large number of parameters (at least 20), whose arbitrary tuning allows a wide range of possible experimental predictions. This fact has discouraged many experimentalists, since any experimental limit would appear to be always avoidable by suitable tuning of the many parameters. These many-parameter models lack theoretical motivation, whereas, theoretically well-motivated supersymmetric models have invariably much fewer parameters and can be straightforwardly falsified. In this context we consider unified supergravity models with universal soft supersymmetry breaking and radiative electroweak symmetry breaking, thus restricting the number of parameters to four. To sharpen the predictions even more, we also consider string-inspired no-scale SU(5)×U(1) supergravity, which can be described in terms of two parameters, or even only one parameter in its strict version.

Calculations of $B(b \to s\gamma)$ in supergravity models have been performed in Refs. [8,11,14–16] under various assumptions, such as radiative electroweak breaking using the tree-level Higgs potential [8,14,15], or imposing relations among the supersymmetry breaking parameters (such as $B = A - 1$ [8,14–16], or $B = 2$ [16], or $m_0 = A = 0$ [11]). In this paper we reexamine the $B(b \to s\gamma)$ calculation in string-inspired no-scale SU(5)×U(1) supergravity and in the minimal SU(5) supergravity model. For a direct comparison with other possible supergravity models, we extend our calculations to a large class of generic four-parameter supergravity

models.

It is found that $B(b \to s\gamma)$ can be enhanced in supersymmetric models in the presence of light sparticles, and more importantly for large values of the ratio of Higgs vacuum expectation values ($\tan\beta$). Indeed, large values of $\tan\beta$ enhance the down-type quark and charged lepton Yukawa couplings, in particular $\lambda_b \propto 1/\cos\beta \sim \tan\beta$ for large $\tan\beta$. (An analogous effect also enhances the supersymmetric contribution to the anomalous magnetic moment of the muon, through a large muon Yukawa coupling [17].) We find that when the various decay amplitudes have the same sign, this enhancement results in new upper bounds on $\tan\beta$, assuming a supersymmetric spectrum below the TeV scale.

This paper is organized as follows. In Sec. II we describe briefly the models under study. In Sec. III we discuss the expression used to calculate $B(b \to s\gamma)$ and the various uncertainties involved. In Sec. IV we present and discuss our results, and obtain new upper bounds on $\tan\beta$ using the present experimentally allowed range. We also delineate the regions of parameter space which are consistent with the standard model prediction, and explore the m_t dependence of our results. These show a strong preference for one sign of the Higgs mixing parameter μ. Finally, in Sec. V we summarize our conclusions.

II. THE SUPERGRAVITY MODELS

We consider unified supergravity models with universal soft supersymmetry breaking and radiative breaking of the electroweak symmetry. At the unification scale the models are described by four soft-supersymmetry-breaking parameters: the universal gaugino mass ($m_{1/2}$), the universal scalar mass (m_0), the universal trilinear scalar coupling (A), and the bilinear scalar coupling (B); and by four superpotential couplings: the Higgs mixing parameter μ, and the third-generation Yukawa couplings ($\lambda_t, \lambda_b, \lambda_\tau$). At low energies there also arises the ratio of Higgs vacuum expectation values ($\tan\beta$). The renormalization group equations connect the values of the parameters at the low- and high-energy scales. These nine parameters reduce to five by the imposition of a good minimum of the one-loop effective Higgs potential at the electroweak scale (one condition for each of the two real scalar Higgs fields; $|\mu|$ and B are determined), and by trading the set $(\lambda_t, \lambda_b, \lambda_\tau, \tan\beta)$ for $(m_t, m_b, m_\tau, \tan\beta)$ and using the known values of m_b and m_τ. Once the five independent parameters $(m_{1/2}, m_0, A, m_t, \tan\beta)$ are specified, one can obtain the whole low-energy spectrum and enforce all the known bounds on sparticle and Higgs-boson masses. We note that, unlike Refs. [8,14–16], we do not impose the additional restriction $B = A - 1$ at the unification scale. For recent reviews of this procedure, see, e.g., Ref. [18].

For a fixed value of the top-quark mass, we therefore have a family of four-parameter supersymmetric models. We further specify this set as $(m_{\chi_1^\pm}, \xi_0, \xi_A, \tan\beta)$, where $m_{\chi_1^\pm} \propto m_{1/2}$ and we have defined $\xi_0 \equiv m_0/m_{1/2}$ and $\xi_A = A/m_{1/2}$. This type of ratios of soft-supersymmetry-breaking parameters occurs naturally in various string-inspired supersymmetry-breaking scenarios (see below). In what follows, we consider continuous values of $m_{\chi_1^\pm}$ and a grid of values for the other three parameters: $\tan\beta = 2$–40 (in steps of 2); $\xi_0 = 0, 1, 2, 5, 10$; $\xi_A = 0, +\xi_0, -\xi_0$. For reference, the average squark mass is related to the gluino mass as follows: $m_{\tilde{q}} \approx (m_{\tilde{g}}/2.9)\sqrt{6+\xi_0^2}$, i.e., $m_{\tilde{q}} \approx (0.8, 0.9, 1.1, 1.9, 3.6)m_{\tilde{g}}$ for $\xi_0 = 0, 1, 2, 5, 10$.

Within this class of four-parameter models we also consider the minimal SU(5) supergravity model, where one finds two additional constraints: a sufficiently long proton lifetime [19] and a sufficiently small neutralino relic density [20]. In what follows, the proton lifetime has been calculated assuming that the Higgs-triplet mass does not exceed ten times the unification scale (which implies $\tan\beta \lesssim 10$ and $\xi_0 \gtrsim 4$). These combined constraints restrict the parameter space to $m_{\chi_1^\pm} \lesssim 120$ GeV and $m_{\tilde{g}} \lesssim 400$ GeV.

An even more predictive class of supersymmetric models is obtained by considering no-scale SU(5)×U(1) supergravity [21]. In this case, unification occurs at the string scale $M_{\rm string} \sim 10^{18}$ GeV, and one assumes string-inspired relations among the soft-supersymmetry-breaking parameters resulting in two scenarios: (i) the *moduli* scenario with $m_0 = A = 0$ [22,23], and (ii) the *dilaton* scenario with $m_0 = \frac{1}{\sqrt{3}} m_{1/2}, A = -m_{1/2}$ [24]. In either case one obtains two-parameter models $(m_{\chi_1^\pm}, \tan\beta)$. These two scenarios have been studied in detail in Refs. [25,26] respectively. One finds that the proton decay and cosmological constraints are satisfied automatically in both scenarios. We also consider a "strict" version of these scenarios, where the parameter B at the unification scale is also specified: (i) $B(M_U) = 0$ (moduli scenario or "strict no-scale"), and (ii) $B(M_U) = 2m_0$ (dilaton scenario or "special dilaton"). The specification of $B(M_U)$ allows one to determine $\tan\beta$: $\tan\beta = \tan\beta(m_{\chi_1^\pm})$, i.e., one obtains one-parameter models. Moreover, the sign of μ is restricted to be negative in both these cases.[1]

In our calculations we have taken the "running" top-quark mass to be $m_t \equiv m_t(m_t) = 150$ GeV. (In Sec. IV D we comment on the m_t-dependence of our results.) This parameter is related to the experimentally observable "pole" mass by [27]

$$m_t^{\rm pole} = m_t(m_t)\left[1 + \frac{4}{3}\frac{\alpha_s(m_t)}{\pi} + K_t\left(\frac{\alpha_s(m_t)}{\pi}\right)^2\right], \quad (1)$$

where

$$K_t = 16.11 - 1.04\sum_{m_{q_i}<m_t}\left(1 - \frac{m_{q_i}}{m_t}\right) \approx 11\ . \quad (2)$$

[1] In the "strict no-scale" case both signs of μ are in principle allowed. However, $\mu > 0$ can occur only for $m_t \lesssim 135$ GeV which appears quite disfavored by the latest experimental information on the top-quark mass.

Thus we obtain $m_t^{\rm pole} \approx 1.07 m_t$, and our choice $m_t = 150$ GeV corresponds to $m_t^{\rm pole} = 160$ GeV, which is in good agreement with the latest fit to all data $m_t = 162 \pm 9$ GeV [28].

When large values of $\tan\beta$ are allowed, we also consider the constraints from the anomalous magnetic moment of the muon. This constraint is not as restrictive as that from $B(b \to s\gamma)$, but nonetheless can exclude additional points in parameter space for $\mu < 0$. Also, in the generic four-parameter models, the cosmological constraint of a not-too-large neutralino relic density becomes quite restrictive for $\xi \gtrsim 2$ and not-too-large values of $\tan\beta$ [29]. This constraint is also imposed below.

In what follows we will present our results in a way that makes apparent the impact of $B(b \to s\gamma)$ on the parameter space, irrespective of any additional applicable constraints, and also when all constraints are combined.

III. FORMULA AND UNCERTAINTIES

We use the following leading-order (LO) expression for the branching ratio [10]:

$$\frac{B(b \to s\gamma)}{B(b \to ce\bar{\nu})} = \frac{6\alpha}{\pi} \frac{|V_{ts}^* V_{tb}|^2}{|V_{cb}|^2} \frac{1}{g(m_c/m_b)} \left[\eta^{16/23} A_\gamma + \frac{8}{3}(\eta^{14/23} - \eta^{16/23}) A_g + C \right]^2 , \quad (3)$$

where $\eta = \alpha_s(M_Z)/\alpha_s(Q), g$ is the phase-space factor $g(x) = 1 - 8x^2 + 8x^6 - x^8 - 24x^4 \ln x, C = C(Q)$ is a QCD correction factor, and Q is the renormalization scale. The A_γ, A_g are the coefficients of the effective $bs\gamma$ and bsg penguin operators evaluated at the scale M_Z. These coefficients receive five contributions [8] from: the $t - W^\pm$ loop, the $t - H^\pm$ loop, the $\chi^\pm_{1,2} - \tilde{t}_{1,2}$ (the "chargino" contribution), the $\tilde{g} - \tilde{q}$ loop (the "gluino" contribution), and the $\chi^0_i - \tilde{q}$ loop (the "neutralino" contribution). The gluino and neutralino contributions are much smaller than the chargino contribution [8,15] and are neglected in the following. In fact, it is when the chargino contribution becomes large (for light sparticles and large $\tan\beta$) that $B(b \to s\gamma)$ can greatly deviate from the standard model result. As only the top squarks ($\tilde{t}_{1,2}$) are significantly split, in the chargino contribution we ignore the other squark splittings. The top-squark splitting affects the magnitude of the chargino contribution, and for fixed m_t it depends mostly on the parameter A (or at low energies on A_t). Expressions for A_γ, A_g can be found in Ref. [10].

As is, this expression for $B(b \to s\gamma)$ is subject to partially unknown next-to-leading-order (NLO) QCD corrections. It has been recently shown [6,7] that the magnitude of the NLO corrections can be estimated by allowing the renormalization scale Q to vary between $m_b/2$ and $2m_b$. A complete NLO calculation would yield an expression with a much milder Q dependence, with the expectation that the NLO value for $B(b \to s\gamma)$ would be obtained from the LO expression for a choice of Q in the $m_b/2 \to 2m_b$ interval. Therefore, in what follows, we use the LO expression[2] in Eq. (3) and obtain a range of values for each point in parameter space by taking $m_b/2 < Q < 2m_b$, with $m_b = 4.65$ GeV. Consistent with this procedure we use the one-loop approximation to the running of the strong coupling, i.e.,

$$\eta = \alpha_s(M_Z)/\alpha_s(Q) = 1 - 22/3[\alpha_s(M_Z)/2\pi]\ln(M_Z/Q)$$

(we take $\alpha_s(M_Z) = 0.120$). In evaluating Eq. (3) we also take $|V_{ts}^* V_{tb}|^2/|V_{cb}|^2 = 0.95 \pm 0.04$, $m_c/m_b = 0.316 \pm 0.013$, and $B(b \to ce\bar{\nu}) = 10.7\%$ [7]. Finally $C = C(Q) = \sum_{i=1}^8 b_i \eta^{d_i}$, with the b_i, d_i coefficients given in Ref. [10]. For $Q = m_b/2, m_b, 2m_b$ we obtain $\eta = 0.486, 0.583, 0.680$ and $C = -0.208, -0.160, -0.117$. Following the above procedure, but keeping only the $t - W^\pm$ contribution to A_γ, A_g we obtain the following range for the standard model contribution

$$B(b \to s\gamma)_{\rm SM} = (1.97\text{–}3.10) \times 10^{-4} . \quad (4)$$

The above discussion of QCD corrections implicitly assumes that only two mass scales are involved in the problem: the high electroweak scale and the low b-quark mass scale. In practice the supersymmetric particles have a spectrum that can be spread above or below the electroweak scale. Recently there has appeared the first study of QCD corrections to $B(b \to s\gamma)$ in the supersymmetric case [30], which shows that the running from the electroweak scale down to the b-quark mass scale gives the largest QCD correction. However, a proper treatment of the supersymmetric spectrum at the high scale may produce non-negligible effects. We hope that the scale uncertainty that we have introduced above is large enough to effectively encompass the supersymmetric high scale uncertainty as well.

IV. RESULTS AND DISCUSSION

We now present the results of the calculations of $B(b \to s\gamma)$ for the various supergravity models under consideration. We start by examining the results in SU(5)×U(1) supergravity and the minimal SU(5) supergravity model, and then extend our calculations to the generic four-parameter models described in Sec. II.

[2] In Eq. (3) we have removed from the denominator the QCD correction factor for the semileptonic decay that was used in our previous analyses [11]. This factor has to be removed in order to obtain a true LO expression, without any NLO contributions.

A. SU(5)×U(1) supergravity

The calculated values of $B(b \to s\gamma)$ in the moduli and dilaton scenarios are shown in Figs. 1 and 2 respectively, for selected values of $\tan\beta$; consistency of the model entails an upper limit of $\tan\beta \lesssim 26(40)$ in the moduli (dilaton) scenario. In these and other figures showing values of $B(b \to s\gamma)$ we take $Q = m_b$ as a "central" value. The full uncertainty range is considered when discussing whether or not given points in parameter space are excluded. In Figs. 1 and 2 the arrows point into the experimentally allowed region and the dashed lines (SM) delimit the standard model prediction. For $\mu > 0$ the values of $B(b \to s\gamma)$ increase steadily with increasing $\tan\beta$ and eventually fall outside the experimentally allowed region for all values of $m_{\chi_1^\pm}$. (The largest values of $m_{\chi_1^\pm}$ shown correspond to $m_{\tilde{q}}, m_{\tilde{g}} \approx 1$ TeV.)

For $\mu < 0$ the $\tan\beta$-dependence is different. One sees that $B(b \to s\gamma)$ can be suppressed much below the standard model result. This behavior was first noticed in Ref. [11] and simply shows that the various amplitudes and QCD correction factors in Eq. (3) conspire to produce a cancellation. This phenomenon has been since explained in Refs. [12,16]. The idea is that the chargino contribution to A_γ can have the same sign (negative) or opposite sign (positive) compared to the $t - W^\pm$ and $t - H^+$ contributions which are always negative. In fact, the sign of the chargino contribution is determined by the product $\theta_{\tilde{t}}\mu$: positive for $\theta_{\tilde{t}}\mu < 0$ and negative for $\theta_{\tilde{t}}\mu > 0$ [12].[3] Here $\theta_{\tilde{t}}$ is the top-squark mixing angle, $\theta_{\tilde{t}} \approx \pi/4$ in this approximation to the chargino contribution [10]. Therefore, constructive interference occurs for $\mu > 0$ and destructive interference occurs for $\mu < 0$, as evident in Figs. 1 and 2. Figure 2 also shows that despite the destructive interference, for $\mu < 0$ and sufficiently large values of $\tan\beta$, an enhancement can occur for light chargino masses because the chargino contribution overwhelms the other two contributions.

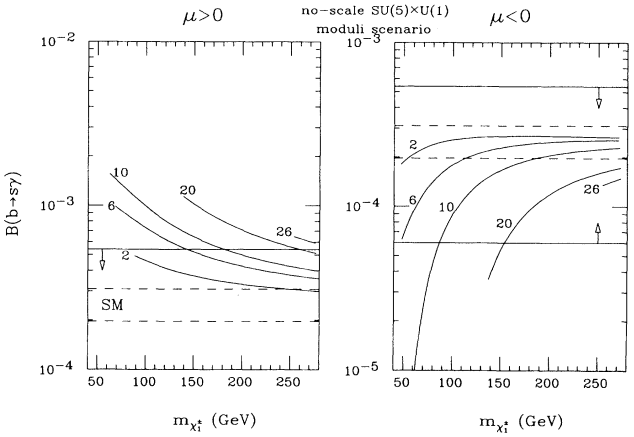

FIG. 1. The calculated "central" values of $B(b \to s\gamma)$ in no-scale SU(5)×U(1) supergravity-moduli scenario, for representative values of $\tan\beta$. The arrows point into the experimentally allowed region. The dashed lines delimit the standard model range.

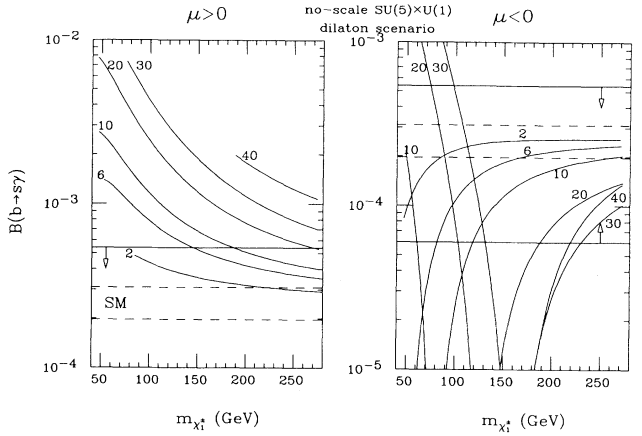

FIG. 2. The calculated "central" values of $B(b \to s\gamma)$ in no-scale SU(5)×U(1) supergravity-dilaton scenario, for representative values of $\tan\beta$. The arrows point into the experimentally allowed region. The dashed lines delimit the standard model range.

To better appreciate the impact of the present experimental limit on $B(b \to s\gamma)$, we classify points in parameter space into three categories.

Excluded points have $B(b \to s\gamma)$ ranges which do not overlap with the present experimental allowed range [i.e., $(0.6\text{–}5.4)\times10^{-4}$]. This conservative constraint (i.e., use of theoretical ranges rather than central values) is imposed so that our excluded points are not dependent on presently unknown NLO QCD corrections.

Preferred points have $B(b \to s\gamma)$ ranges which overlap with the standard model range [i.e., $(1.97\text{–}3.10)\times10^{-4}$].

Ok points are neither "excluded" nor "preferred," and may become "excluded" if new CLEO data are consistent with the standard model prediction.

The two-dimensional parameter spaces for the moduli and dilaton scenarios are shown in Figs. 3 and 4 respectively. In these figures crosses (×) represent "excluded" points, diamonds (◇) represent "preferred" points, and dots (·) represent "Ok" points. The vertical dashed line at $m_{\chi_1^\pm} = 100$ GeV in these and following parameter space plots indicates the approximate reach of the CERN e^+e^- collider LEPII for chargino masses. As anticipated, there are many "excluded" points for $\mu > 0$, especially as $\tan\beta$ gets large. Also, the "preferred" points occur largely for $\mu < 0$, signaling the ability of the $B(b \to s\gamma)$ constraint to possibly select the sign of μ.

For sufficiently large values of $\tan\beta$, the anomalous magnetic moment of the muon $(g-2)_\mu$ can be constraining as well. We have calculated this quantity as in Ref. [17] and denote excluded points (i.e., points for which $\frac{1}{2}(g-2)_\mu^{\rm SUSY}$ falls outside the experimentally allowed

[3] Our sign convention for μ is opposite to that in Ref. [12], but the same as that in Ref. [16].

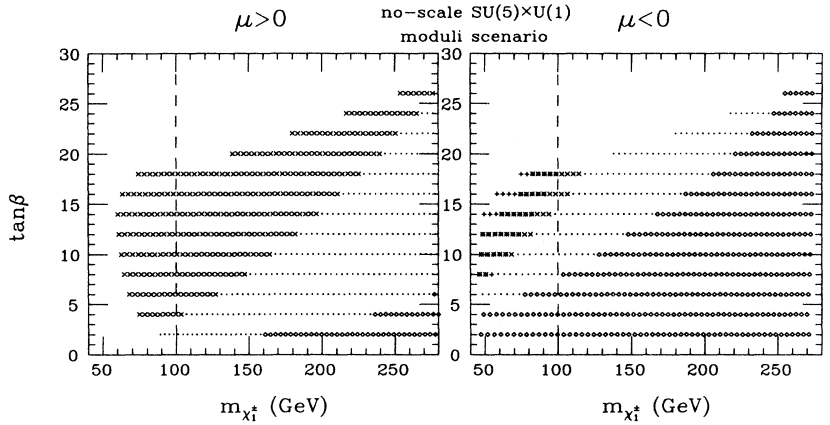

FIG. 3. The two-dimensional parameter space of no-scale SU(5)×U(1) supergravity-moduli scenario. Points excluded by $B(b \to s\gamma)$ are denoted by crosses (×), those consistent with the standard model prediction are denoted by diamonds (◇), and the rest are denoted by dots (·). Plusses (+) indicate points excluded by $(g-2)_\mu$, whereas asterisks (∗) indicate points excluded by both constraints.

range of $-13.2 \times 10^{-9} \to 20.8 \times 10^{-9}$ [17]) by plusses (+) in Figs. 3 and 4. We have only shown these excluded points for $\mu < 0$, since for $\mu > 0$ the $(g-2)_\mu$ constraint does not exclude any points which are not excluded by the $B(b \to s\gamma)$ constraint. The effect of this constraint is most noticeable in the dilaton scenario (Fig. 4) where "preferred" points which are thusly excluded appear as the overlap of a plus sign and a clear diamond (i.e., "filled" diamonds) for $\tan\beta = 10$–32 and $m_{\chi_1^\pm} \lesssim 100$ GeV. Points excluded by both $B(b \to s\gamma)$ and $(g-2)_\mu$ appear as the overlap of a plus sign and a cross, i.e., as asterisks (∗).

Overall, the $B(b \to s\gamma)$ constraint is quite restrictive. Statistically we have the following distribution of fractions of parameter space:

	Moduli		Dilaton	
	$\mu > 0$	$\mu < 0$	$\mu > 0$	$\mu < 0$
Excluded	48%	7%	73%	21%
Preferred	9%	66%	6%	33%
Ok	43%	27%	21%	46%

Note that should the new CLEO data be consistent with the standard model prediction, then only the "preferred" points would survive. For $\mu > 0$ this is 9(6)% of all the points in parameter space in the moduli (dilaton) scenario, whereas for $\mu < 0$ one would still have $\frac{2}{3}$ ($\frac{1}{3}$) of the points allowed—an overwhelming inclination towards $\mu < 0$.

From Figs. 3 and 4 one can also see that for $\mu > 0$ there is an upper bound on $\tan\beta$: $\tan\beta \lesssim 25$. For the subset of "preferred" points this bound drops to $\tan\beta \lesssim 6$. We should add that these bounds can be evaded by demanding sufficiently heavy sparticles (in the multi-TeV range), but then supersymmetry would lose most of its motivation. There are no analogous bounds for $\mu < 0$.

Note that the "preferred" points for $\mu > 0$ entail a supersymmetric spectrum inaccessible to direct searches at LEPII (i.e., $m_{\chi_1^\pm} \gtrsim 150$ GeV, $m_{\tilde{g}} \approx m_{\tilde{q}} \gtrsim 500$ GeV). In contrast, some of the "preferred" points for $\mu < 0$ would be directly accessible at LEPII.

In the strict no-scale case, the one-parameter models allow one to plot $B(b \to s\gamma)$ as a function of $m_{\chi_1^\pm}$ only. These values are shown in Fig. 5. Since in both cases $\mu < 0$, the plots are reminiscent of the $\mu < 0$ plots in the general moduli and dilaton scenarios. In Fig. 6 we show the corresponding one-dimensional parameter spaces, where one can see that in the dilaton scenario there are no excluded points. The constraint from $(g-2)_\mu$ is ineffective in the dilaton scenario and does not exclude any further points in the moduli scenario. Figure 6 shows the interest of working with a theory where all predictions are given in terms of only one parameter. For example, a measurement of $m_{\chi_1^\pm}$ would immediately de-

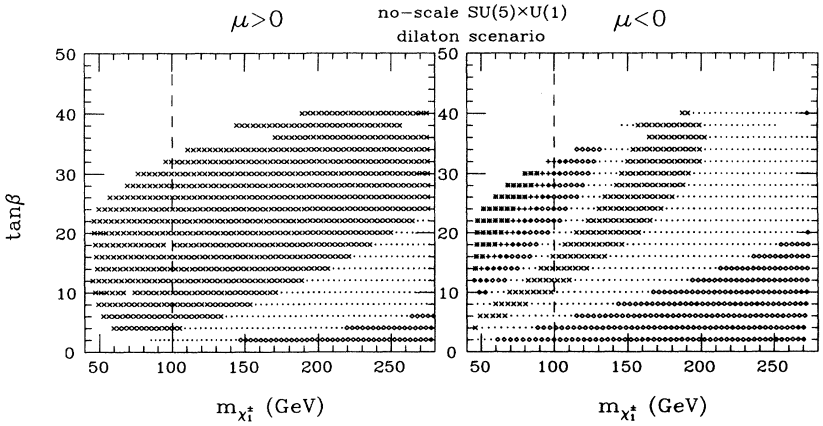

FIG. 4. The two-dimensional parameter space of no-scale SU(5)×U(1) supergravity-dilaton scenario. Points excluded by $B(b \to s\gamma)$ are denoted by crosses (×), those consistent with the standard model prediction are denoted by diamonds (◇), and the rest are denoted by dots (·). Filled diamonds and plusses (+) indicate points excluded by $(g-2)_\mu$, whereas asterisks (∗) indicate points excluded by both constraints.

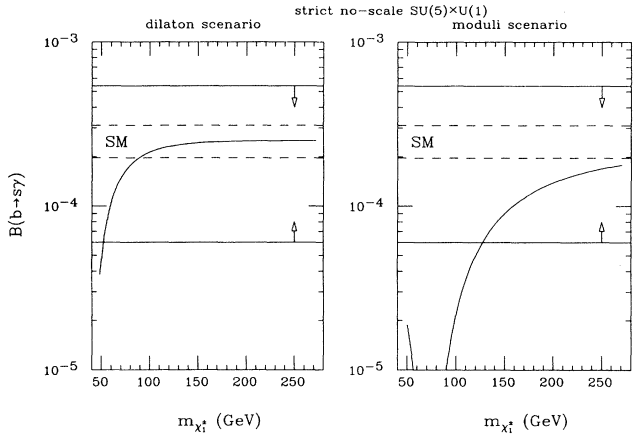

FIG. 5. The calculated "central" values of $B(b \to s\gamma)$ in strict no-scale SU(5)×U(1) supergravity-moduli and dilaton scenarios. The arrows point into the experimentally allowed region. The dashed lines delimit the standard model range.

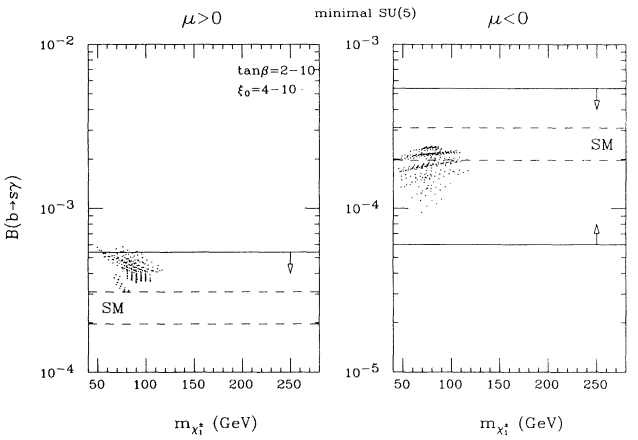

FIG. 7. The calculated "central" values of $B(b \to s\gamma)$ in the minimal SU(5) supergravity model. The constraints from proton decay and cosmology restrict the parameter space as indicated. The arrows point into the experimentally allowed region. The dashed lines delimit the standard model range.

termine $\tan\beta$. Also, if it is found that $2 \lesssim \tan\beta \lesssim 12$ or $\tan\beta \gtrsim 19$ are preferred, then this one-parameter theory should be abandoned.

B. Minimal SU(5) supergravity

As described in Sec. 2, in the case of the minimal SU(5) supergravity model we constrain the four-dimensional parameter space by the requirements of proton decay and cosmology. These entail $\tan\beta \lesssim 10$ and $\xi_0 \gtrsim 4$. In Fig. 7 we show the calculated central values of $B(b \to s\gamma)$ in this case. Because the values of $\tan\beta$ are not allowed to be large we do not expect large deviations from the standard model prediction, as seen in the figure. Nonetheless, there are deviations, especially for $\mu > 0$. Given the uncertainties in the calculation of $B(b \to s\gamma)$ described in Sec. III, we find no "excluded" points, and the following distribution of fractions of parameter space:

	Minimal SU(5)	
	$\mu > 0$	$\mu < 0$
Excluded	0%	0%
Preferred	11%	93%
Ok	89%	7%

Again we see a strong tendency among the "preferred" points towards $\mu < 0$. Moreover, for $\mu > 0 (\mu < 0)$ "preferred" points exist only for $\tan\beta \lesssim 4(8)$.

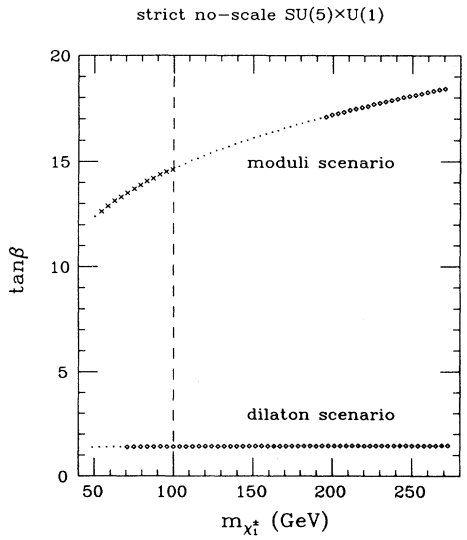

FIG. 6. The one-dimensional parameter space of strict no-scale SU(5)×U(1) supergravity-moduli and dilaton scenarios. Points excluded by $B(b \to s\gamma)$ are denoted by crosses (×), those consistent with the standard model prediction are denoted by diamonds (◇), and the rest are denoted by dots (·).

C. Generic supergravity models

For completeness, we now turn to the generic four-parameter supergravity models. These models could be viewed as essentially SU(5) supergravity models where the constraint from proton decay is simply ignored (the cosmological constraint is not neglected). In the spirit of Ref. [29], we consider these models to see if $b \to s\gamma$ could shed some light on the structure of the soft supersymmetry breaking sector in supergravity or superstring models. As mentioned in Sec. II, we have considered continuous values of $m_{\chi_1^\pm}$ and a grid of values for the other three parameters: $\tan\beta$ = 2–40 (in steps of 2); $\xi_0 = 0, 1, 2, 5, 10$; $\xi_A = 0, +\xi_0, -\xi_0$. We will concentrate on $\xi_0 = 1, 2$ since the SU(5)×U(1) scenarios correspond approximately to $\xi_0 = 0, \frac{1}{\sqrt{3}}$, and larger values of ξ_0 lead to increasingly heavier sparticle masses. We will comment on the $\xi_0 = 5, 10$ cases later. In Figs. 8 and 9 we

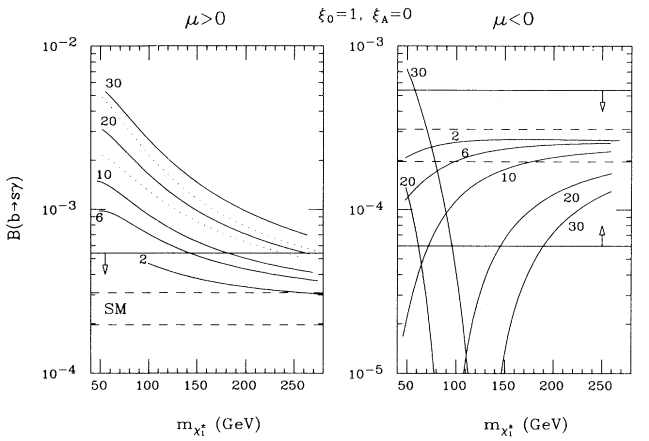

FIG. 8. The calculated "central" values of $B(b \to s\gamma)$ in the generic supergravity model for $\xi_0 = 1$ and $\xi_A = 0$, for representative values of $\tan\beta$. The dotted curve above (below) the $\tan\beta = 20$ curve for $\mu > 0$ corresponds to $\xi_A = -1(+1)$. The arrows point into the experimentally allowed region. The dashed lines delimit the standard model range.

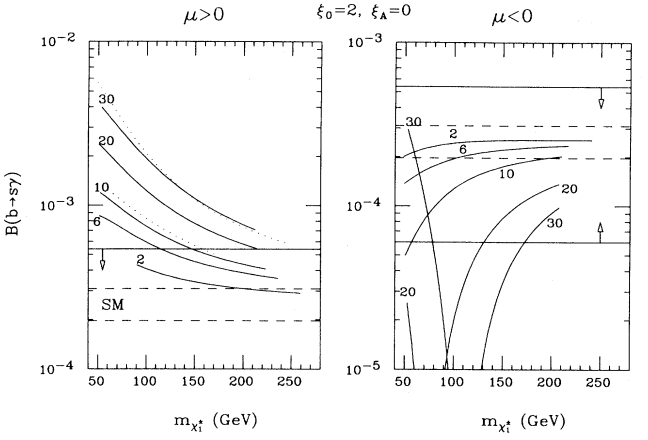

FIG. 9. The calculated "central" values of $B(b \to s\gamma)$ in the generic supergravity model for $\xi_0 = 2$ and $\xi_A = 0$, for representative values of $\tan\beta$. The dotted curve above (below) the $\tan\beta = 20$ curve for $\mu > 0$ corresponds to $\xi_A = -2(+2)$. The arrows point into the experimentally allowed region. The dashed lines delimit the standard model range.

show $B(b \to s\gamma)$ for $\xi_0 = 1$ and 2, respectively, for representative values of $\tan\beta$. These curves are for $\xi_A = 0$. The effect of different choices for ξ_A is shown by the dotted lines in these figures (for the same $\tan\beta = 20$ and ξ_0 choice): $\xi_A < 0$ enhances $B(b \to s\gamma)$ since negative A values drive A_t at low energies to even more negative values and thus larger $\tilde{t}_{1,2}$ splittings. Increasing ξ_0 from 1 to 2 has the expected effect of decreasing $B(b \to s\gamma)$.

For fixed values of ξ_0 and ξ_A we can plot the parameter space in the $(m_{\chi_1^\pm}, \tan\beta)$ plane, as was done in the SU(5)×U(1) supergravity case. The points in parameter space are again classified into "excluded," "preferred," and "Ok" as discussed in Sec. IV A. These plots for $\xi_0 = 1, 2$ and $\xi_A = 0, +\xi_0, -\xi_0$ are shown in Figs. 10 and 11.

For $\xi_0 = 1$ the $(g-2)_\mu$ constraint excludes additional points in parameter space for $\mu < 0$. These appear as filled diamonds and plusses (+) in Fig. 10. The effect of ξ_A discussed above is also evident in this figure, i.e., for $\xi_A = -1$ one sees that $B(b \to s\gamma)$ is enhanced. The island of "preferred" points for $\mu < 0, m_{\chi_1^\pm} \lesssim 100$ GeV and not-so-small values of $\tan\beta$ corresponds to the curves in Fig. 8 which "bounce back" for light chargino masses. Note that most of these points are in fact excluded by the $(g-2)_\mu$ constraint. The cosmological constraint is unrestrictive for $\xi_0 = 1$.

For $\xi_0 = 2$ the $(g-2)_\mu$ constraint does not exclude any points in parameter space which are not also excluded by the $B(b \to s\gamma)$ constraint. However the cosmological constraint becomes important and excludes points denoted by filled diamonds and plusses in Fig. 11. Note that this constraint excludes most (if not all) of the (few) "preferred" points for $\mu > 0$. The right boundary of the parameter space corresponds to the squarks at 1 TeV. The position of this boundary as a function of $m_{\chi_1^\pm}$ depends on ξ_A because A affects the calculation of μ, which in turn affects the value of $m_{\chi_1^\pm}$.

In analogy with the discussion for the previous models, statistically we have the following distribution of fractions of parameter space (excluding the cosmological constraint):

	$\xi_0 = 1$						$\xi_0 = 2$					
	$\mu > 0$			$\mu < 0$			$\mu > 0$			$\mu < 0$		
ξ_A	+1	0	−1	+1	0	−1	+2	0	−2	+2	0	−2
Excluded	70%	74%	76%	12%	15%	20%	62%	72%	78%	9%	17%	27%
Preferred	4%	4%	4%	53%	43%	36%	7%	6%	5%	51%	36%	29%
Ok	26%	22%	20%	35%	43%	44%	31%	23%	17%	40%	47%	44%

In this case we again see the marked tendency of the "preferred" points for $\mu < 0$, i.e., only few percent of the points for $\mu > 0$ are "preferred." Including the cosmological constraint makes this tendency even more pronounced. From Figs. 10 and 11 we also notice the upper bound on $\tan\beta$ for $\mu > 0$: $\tan\beta \lesssim 25$ in general and $\tan\beta \lesssim 6$ for the "preferred" points.

For $\xi_0 = 5, 10$ the parameter space is generally quite

limited in the $\tan\beta$ direction, i.e., $\tan\beta \lesssim 4(2)$ for $\xi_0 = 5(10)$. Higher values of $\tan\beta$ are inconsistent with radiative electroweak symmetry breaking. Using the tree-level scalar potential such values of $\tan\beta$ give $\mu^2 < 0$. In our calculations (using the one-loop effective potential) no minimum can be found. This limitation on $\tan\beta$ can be circumvented for sufficiently negative values of ξ_A, e.g., $\xi_A = -5$ (-10) for $\xi_0 = 5$ (10). In any event, the qualitative results obtained above for the strong tendency of the "preferred" points towards $\mu < 0$, holds also for large values of ξ_0. The cosmological constraint exacerbates this tendency. For $\xi_0 = 10$ basically all points in parameter space for $\mu > 0$ are excluded; for $\mu < 0$ a few survive.

D. m_t dependence

Our calculations above have been performed for a fixed value of m_t. Given the present uncertainty on the actual value of m_t, it is appropriate to explore the m_t dependence of our results. In the standard model we obtain

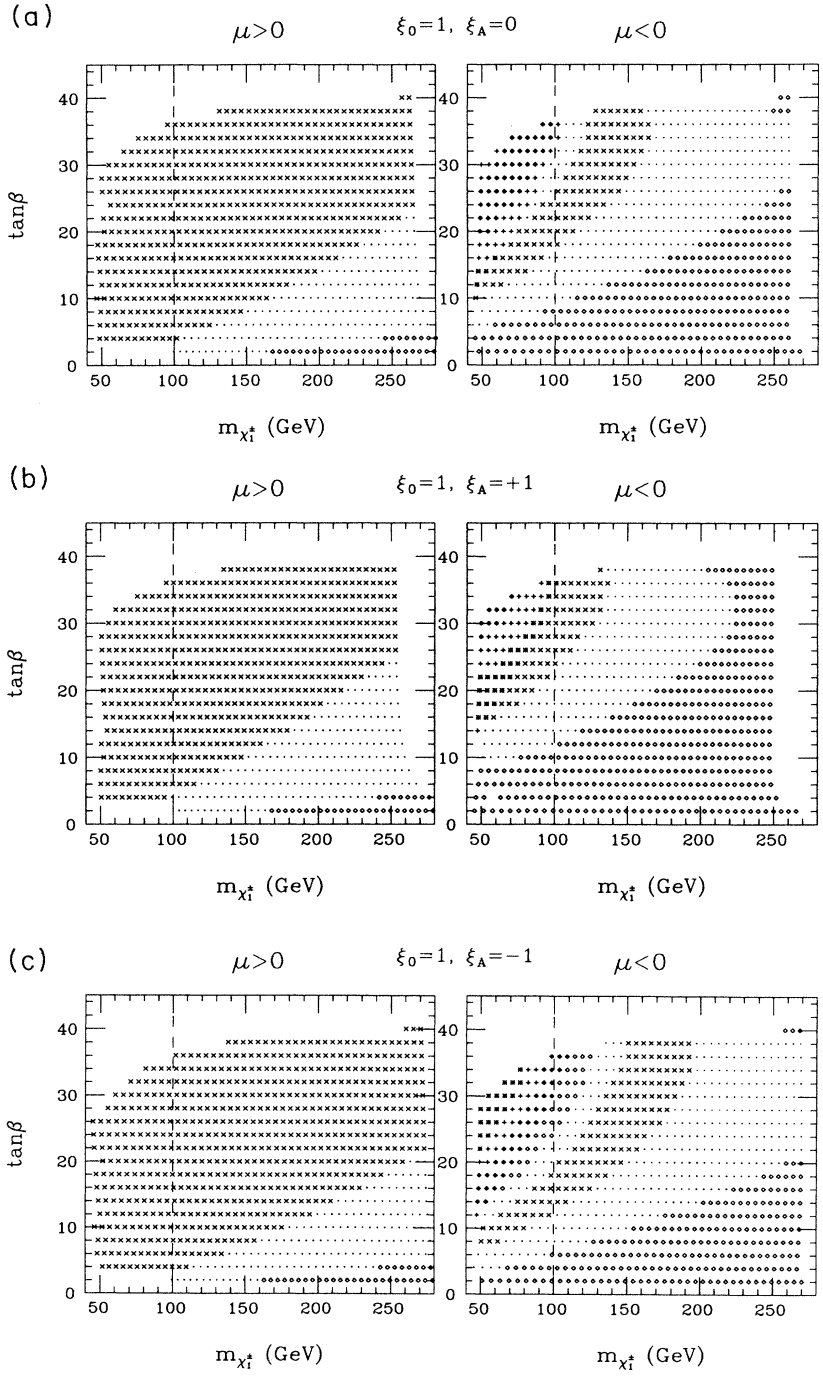

FIG. 10. The parameter space of the generic supergravity model for $\xi_0 = 1$ and (a) $\xi_A = 0$, (b) $\xi_A = +1$, and (c) $\xi_A = -1$. Points excluded by $B(b \to s\gamma)$ are denoted by crosses $(\times)$, those consistent with the standard model prediction are denoted by diamonds $(\diamond)$, and the rest are denoted by dots $(\cdot)$. Filled diamonds and plusses $(+)$ indicate points excluded by $(g-2)_\mu$, whereas asterisks $(*)$ indicate points excluded by both constraints.

the following LO ranges for $B(b \to s\gamma)_{\rm SM}$:

$m_t = 130$ GeV, $B(b \to s\gamma)_{\rm SM} = (1.77\text{–}2.89) \times 10^{-4}$,
$m_t = 150$ GeV, $B(b \to s\gamma)_{\rm SM} = (1.97\text{–}3.10) \times 10^{-4}$,
$m_t = 170$ GeV, $B(b \to s\gamma)_{\rm SM} = (2.15\text{–}3.28) \times 10^{-4}$,
$m_t = 190$ GeV, $B(b \to s\gamma)_{\rm SM} = (2.31\text{–}3.44) \times 10^{-4}$.

These results indicate that a measurement of $B(b \to s\gamma)$ will not give new information on m_t (since all intervals overlap), at least at the LO level. A NLO calculation would be most useful in this regard.

We have also re-done the calculation of $B(b \to s\gamma)$ in SU(5)×U(1) supergravity for various values of m_t. As expected, the m_t dependence is weak. To better quantify this statement, as a function of m_t we have determined the fractions of parameter space which are "preferred":

	Moduli		Dilaton	
m_t	$\mu > 0$	$\mu < 0$	$\mu > 0$	$\mu < 0$
150	9%	66%	6%	33%
160	8%	66%	5%	32%
170	8%	66%	4%	31%
180	2%	67%	1%	28%

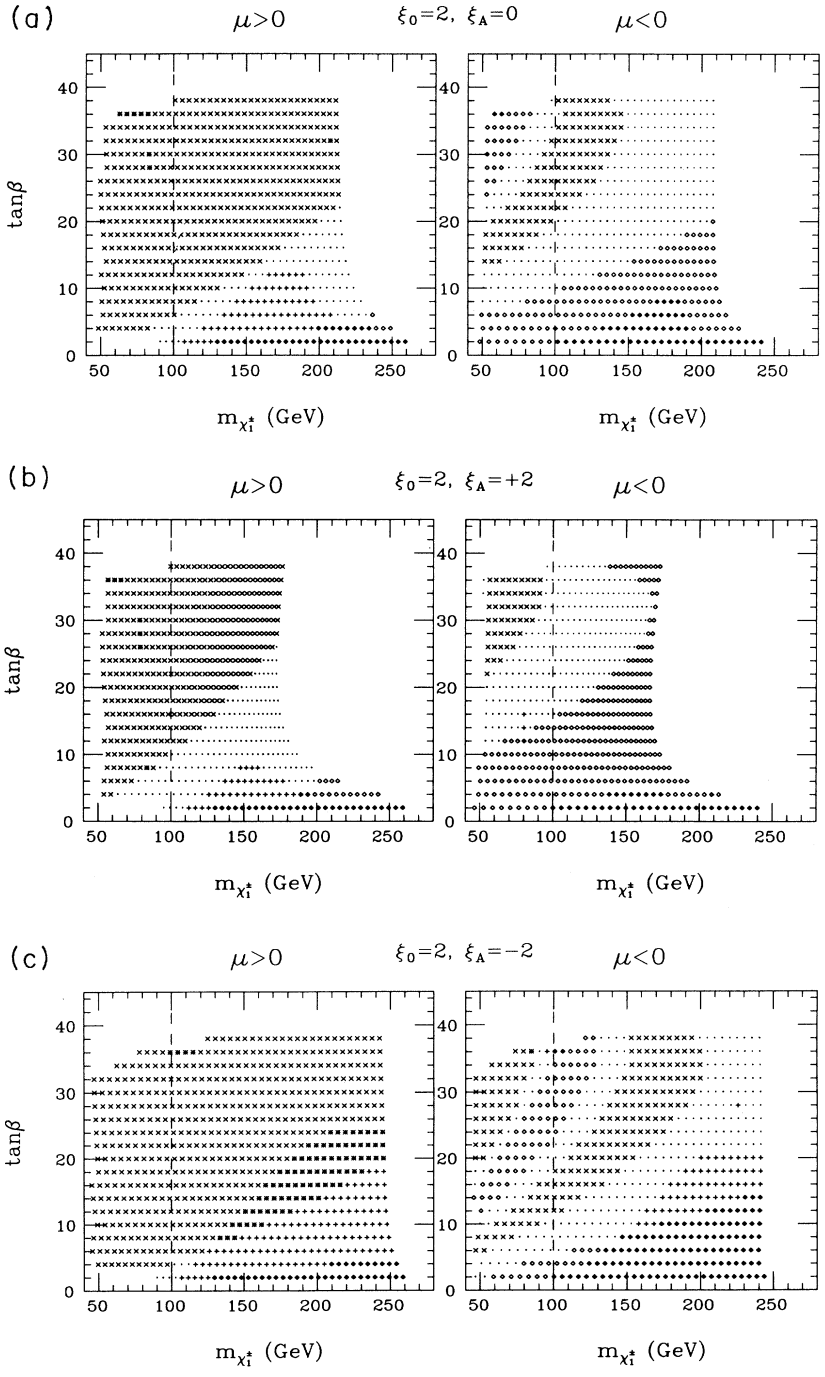

FIG. 11. The parameter space of the generic supergravity model for $\xi_0 = 2$ and (a) $\xi_A = 0$, (b) $\xi_A = +2$, and (c) $\xi_A = -2$. Points excluded by $B(b \to s\gamma)$ are denoted by crosses (×), those consistent with the standard model prediction are denoted by diamonds (◇), and the rest are denoted by dots (·). Filled diamonds and plusses (+) indicate points excluded by the *cosmological* constraint, whereas asterisks (∗) indicate points excluded by both constraints. At the right boundary of the parameter space the squark masses reach 1 TeV.

Except for $m_t = 180$ GeV, the fractions of parameter space which are "preferred" are largely m_t independent. The increased sensitivity for large values of m_t is interesting, although not very useful since for $m_t \gtrsim 190$ GeV the allowed parameter space disappears because of the well known phenomenon of the top-quark Yukawa coupling encountering a Landau pole below the unification scale.

V. CONCLUSIONS

We have explored a variety of supergravity models with universal soft supersymmetry breaking at the unification scale and radiative electroweak symmetry breaking. Accounting for the inherent uncertainties in the $B(b \to s\gamma)$ evaluation, we have nonetheless been able to exclude a good fraction of points in parameter space which differ significantly from the experimentally allowed range. We have also identified "preferred" regions of parameter space which would be singled out should the new CLEO data be consistent with the standard model prediction. These "preferred" regions occur mostly for one sign of $\mu(< 0)$ (when the chargino contribution has opposite sign relative to the standard model contribution). For the other sign of $\mu(> 0)$ one can obtain upper bounds on $\tan\beta$ assuming a sparticle spectrum below the TeV scale.

It is worth noticing that constraints from $b \to s\gamma$ disfavor the large-$\tan\beta$ solution [31] to the unification of the Yukawa couplings ($\lambda_b = \lambda_\tau$) in SU(5)-like theories (although those are already disfavored by proton decay constraints). In the case of SO(10)-like Yukawa unification ($\lambda_t = \lambda_b = \lambda_\tau$), one requires $\tan\beta \sim 50$ [32], which are also disfavored by $b \to s\gamma$ constraints. However, in this case radiative electroweak symmetry breaking is also difficult and it has been suggested [33] that non-universal soft supersymmetry breaking scenarios may be able to solve both these difficulties.

At the moment, $b \to s\gamma$ is the most important constraint on the parameter spaces of supergravity models. This standing is expected to be much re-enforced when the new CLEO data are announced. At this time it will become quite appropriate to re-examine the phenomenological implications of the still-allowed points in parameter space for direct and indirect searches of supersymmetric particles. We close by remarking that contrary to direct production experiments, the $b \to s\gamma$ process can already explore regions of parameter space with "virtual" mass scales all the way up to the TeV scale.

ACKNOWLEDGMENTS

This work was supported in part by DOE grant DE-FG05-91-ER-40633. The work of X.W. has been supported by the World Laboratory.

[1] J. Ellis, S. Kelley, and D. V. Nanopoulos, Phys. Lett. B **249**, 441 (1990); P. Langacker and M.-X. Luo, Phys. Rev. D **44**, 817 (1991); F. Anselmo, L. Cifarelli, A. Peterman, and A. Zichichi, Nuovo Cimento **104A**, 1817 (1991).

[2] E. Thorndike, Bull. Am. Phys. Soc. **38**, 922 (1993); CLEO Collaboration, R. Ammar *et al.*, Phys. Rev. Lett. **71**, 674 (1993).

[3] M. Shifman, A. Vainshtein, and V. Zakharov, Phys. Rev. **18**, 2583 (1978); S. Bertolini, F. Borzumati, and A. Masiero, Phys. Rev. Lett. **59**, 180 (1987); N. Deshpande, P. Lo, J. Trampetic, G. Eilam, and P. Singer, *ibid.* **59**, 183, (1987); B. Grinstein, R. Springer, and M. Wise, Nucl. Phys. **B339**, 269 (1990).

[4] R. Grigjanis, P. J. O'Donnel, M. Sutherland, and H. Navelet, Phys. Lett. B **213**, 355 (1988); **233**, 239 (1989); **237**, 252 (1990); G. Cella, G. Curci, G. Ricciardi, and A. Viceré, *ibid.* **248**, 181 (1990); M. Misiak, *ibid.* **269**, 161 (1991); **321**, 193 1994); Nucl. Phys. **B393**, 23 (1993); K. Adel and Y. P. Yao, Mod. Phys. Lett. A **8**, 1679 (1993); Phys. Rev. D **49**, 4945 (1994).

[5] A. Ali and C. Greub, Phys. Lett. B **293**, 226 (1992); Z. Phys. C **60**, 433 (1993).

[6] A. Buras, M. Misiak, M. Münz, and S. Pokorski, Nucl. Phys. **B424**, 374 (1994).

[7] M. Ciuchini *et al.*, Phys. Lett. B **334**, 137 (1994), and references therein.

[8] S. Bertolini, F. Borzumati, A. Masiero, and G. Ridolfi, Nucl. Phys. **B353**, 591 (1991).

[9] N. Oshimo, Nucl. Phys. **B404**, 20 (1993).

[10] R. Barbieri and G. Giudice, Phys. Lett. B **309**, 86 (1993).

[11] J. L. Lopez, D. V. Nanopoulos, and G. T. Park, Phys. Rev. D **48**, R974 (1993); J. L. Lopez, D. V. Nanopoulos, G. T. Park, and A. Zichichi, *ibid.* **49**, 355 (1994).

[12] R. Garisto and J. N. Ng, Phys. Lett. B **315**, 372 (1993).

[13] Y. Okada, Phys. Lett. B **315**, 119 (1993).

[14] M. Diaz, Phys. Lett. B **322**, 207 (1994).

[15] F. Borzumati, Z. Phys. C **63**, 291 (1994).

[16] S. Bertolini and F. Vissani, Report No. SISSA 40/94/EP, hep-ph/9403397, 1994 (unpublished).

[17] J. L. Lopez, D. V. Nanopoulos, and X. Wang, Phys. Rev. D **49**, 366 (1994).

[18] J. L. Lopez, D. V. Nanopoulos, and A. Zichichi, Nuovo Cimento Rivista, **17**, 1 (1994).

[19] J. L. Lopez, D. V. Nanopoulos, and H. Pois, Phys. Rev. D **47**, 2468 (1993); J. L. Lopez, D. V. Nanopoulos, H. Pois, and A. Zichichi, Phys. Lett. B **299**, 262 (1993).

[20] J. L. Lopez, D. V. Nanopoulos, and A. Zichichi, Phys. Lett. B **291**, 255 (1992); J. L. Lopez, D. V. Nanopoulos, and K. Yuan, Phys. Rev. D **48**, 2766 (1993).

[21] For a recent review, see "Status of the Superworld: From Theory to Experiment," J. L. Lopez, D. V. Nanopoulos, and A. Zichichi, Prog. Part. Nucl. Phys. **33**, 303 (1994).

[22] J. Ellis, C. Kounnas, and D. V. Nanopoulos, Nucl. Phys. **B241**, 406 (1984); **B247**, 373 (1984); J. Ellis, A. Lahanas, D. V. Nanopoulos, and K. Tamvakis, Phys. Lett. **134B**, 429 (1984).

[23] For a review, see A. B. Lahanas and D. V. Nanopoulos, Phys. Rep. **15**, 1 (1987).

[24] V. Kaplunovsky and J. Louis, Phys. Lett. B **306**, 269 (1993); A. Brignole, L. Ibáñez, and C. Muñoz, Nucl. Phys. B **422**, 125 (1994).

[25] J. L. Lopez, D. V. Nanopoulos, and A. Zichichi, Phys. Rev. D **49**, 343 (1994).

[26] J. L. Lopez, D. V. Nanopoulos, and A. Zichichi, Phys. Lett. B **319**, 451)(1993).

[27] N. Gray, D. Broadhurst, W. Grafe, and K. Schilcher, Z. Phys. **C48**, 673, (1990).

[28] J. Ellis, G. L. Fogli, and E. Lisi, Phys. Lett. B **333**, 118 (1994).

[29] J. L. Lopez, D. V. Nanopoulos, and K. Yuan, Phys. Lett. B **267**, 219 (1991); S. Kelley, J. L. Lopez, D. V. Nanopoulos, H. Pois, and K. Yuan, Phys. Rev. D **47**, 2461 (1993).

[30] H. Anlauf, Report No. SLAC-PUB-6525 hep-ph/9406286, 1994 (unpublished).

[31] See e.g., J. Ellis, S. Kelley, and D. V. Nanopoulos, Nucl. Phys. B **373**, 55 (1992); H. Arason, *et al.*, Phys. Rev. Lett. **67**, 2933 (1991); S. Kelley, J. L. Lopez, and D. V. Nanopoulos, Phys. Lett. B **274**, 387 (1992); V. Barger, M. Berger, and P. Ohman, Phys. Rev. D **47**, 1093 (1993); P. Langacker and N. Polonsky, *ibid.* **49**, 1454 (1994); C. Kolda, L. Roszkowski, J. Wells, and G. Kane, *ibid.* **50**, 3498 (1994).

[32] B. Ananthanarayan, G. Lazarides, and Q. Shafi, Phys. Rev. D **44**, 1613 (1991); S. Kelley, J. L. Lopez, and D. V. Nanopoulos, in Ref. [31].

[33] L. Hall, R. Ratazzi, and U. Sarid, Phys. Rev. D **50**, 7048 (1994); M. Carena, M. Olechowski, S. Pokorski, and C. Wagner, Nucl. Phys. **B426**, 269 (1994).